



Minerva Access is the Institutional Repository of The University of Melbourne

Author/s:

Zou, C;Kallapur, AG;MANZIE, C;Nesic, D

Title:

PDE Battery Model Simplification for SOC and SOH Estimator Design

Date:

2015

Citation:

Zou, C., Kallapur, A. G., MANZIE, C. & Nesic, D. (2015). PDE Battery Model Simplification for SOC and SOH Estimator Design. 54th Annual Conference on Decision and Control (CDC), 54rd IEEE Conference on Decision and Control, CDC 2015, pp.1328-1333. IEEE. <https://doi.org/10.1109/CDC.2015.7402395>.

Persistent Link:

<https://hdl.handle.net/11343/299362>

PDE Battery Model Simplification for SOC and SOH Estimator Design

Changfu Zou, Abhijit G Kallapur, Chris Manzie and Dragan Nešić

Abstract—Accurate knowledge of the battery state-of-charge (SOC) and state-of-health (SOH) is critical for optimal and safe utilisation of the battery. Although the battery system dynamics contain electrochemical, thermal, electrical, and ageing phenomena, most state estimators resort to equivalent circuit models (ECM). These models are often not accurate and are problematic for SOC estimation during an extended range of operations and do not address SOH dynamics. In this paper, starting from an initial high-fidelity Lithium-ion (Li-ion) battery model consisting of a set of partial differential equations (PDE), a recently proposed framework for PDE battery model simplification is employed and one of these obtained models is used for battery state estimation. Model order reduction techniques are then constructively applied to the simplified PDE battery model and resulted in a computationally efficient ordinary differential equation (ODE) model. Based on this obtained ODE model, an extended Kalman filter (EKF) is designed for the estimation of both SOC and SOH. Simulations over 20 cycles show the designed estimator is capable of simultaneously estimating the battery’s SOC in each electrode and SOH.

I. INTRODUCTION

There is an ever-growing trend towards electrifying the powertrain in automotive industry to address the increasingly stringent standards on vehicle emission and fuel economy. Lithium-ion (Li-ion) batteries have been recognised as a leading technology for vehicle applications due to their high energy/power density, long lifetime, no memory effect, and low self-discharge rate. However, to guarantee safe and optimal utilisation of the batteries, accurate knowledge of the state-of-charge (SOC) and state-of-health (SOH) plays a crucial role. Since SOC and SOH are functions of a battery’s internal Li-ion concentrations and capacity fade, respectively, which are unmeasurable states, real-time estimation techniques are necessary for advanced battery management.

Capturing SOC and SOH in the course of a battery’s operation is a very challenging task, since the underlying dynamics involve coupled electrochemical, thermal, electrical, and ageing phenomena in the domains of the negative and positive electrodes and separation [1], [2], [3], [4], [5], [6], and are mathematically governed by a complicated system structure. It consists of a set of coupled nonlinear

partial differential equations (PDE) and is not well suited to traditional model-based controller and estimator design.

In order to overcome issues in model complexity, an alternative way that is extensively used in current battery management systems is to use empirical or equivalent circuit models (ECMs). In [7], [8], the application of an extended Kalman filter (EKF) on several ECMs for battery parameters and SOC estimation is presented. To deal with nonlinearities associated with complex circuit models, unscented Kalman filters (UKF) and particle filters (PF) are designed such as in the work of [9] and [10]. Although these models are relatively simple, they are not very accurate in capturing battery dynamics particularly during high current rates as per [3]. Moreover, ignoring concentration diffusion, Li-ion intercalation, and electrochemical kinetics inside a battery cell, ECMs are unable to provide insights into battery internal information and physical limitations. Hence, algorithms based on this class of models for the whole range of battery operations may be unreliable.

Alternatively, physics-based battery models have been proposed for state estimation. EKFs are developed for SOC estimation based on a single particle model (SPM) [11], [12] in which each battery electrode is assumed to be one lumped particle with only two states representing the system dynamics. To further lower the complexity in PDE battery observer design, a reduced SPM is developed in [13] by ignoring the system dynamics in the positive electrode. However, the effectiveness of these approaches is limited by the accuracy of SPM itself which has been recognised to work only at low current rates as per [3]. Other high order electrochemical model-based estimators are proposed in [14], [15] for SOC estimation without consideration of temperature change and battery degradation. To date, however, estimation algorithms based on physics-based models that capture both SOC and SOH dynamics are still not available.

In this work, an initial high-order model that accurately captures the system dynamical characteristics is proposed for a Li-ion battery. By using analytical methods, a recently proposed framework for PDE model simplification in [2] is employed in simplifying this battery model. This manuscript demonstrates the application of a simplified PDE model from such a framework for the purpose of battery SOC and SOH estimation. Numerical techniques for model order reduction are systematically performed in deriving an appropriate model. Assumptions underlying this model reduction process are explicitly presented and remarked. Based on the reduced model, an EKF is designed for simultaneous SOC and SOH estimation. The estimator’s performance is examined by comprehensive simulations.

This work was partially supported by the National Information Communication Technology, Australia (NICTA), and Australian Research Council through grant FT100100538.

Changfu Zou, Abhijit G Kallapur, and Chris Manzie are with the Department of Mechanical Engineering, University of Melbourne, VIC 3010, Australia. cezou@student.unimelb.edu.au; akallapur,manzie@c@unimelb.edu.au.

Dragan Nešić is with the Department of Electrical and Electronic Engineering, University of Melbourne, VIC 3010, Australia. dnesic@unimelb.edu.au.

II. LI-ION BATTERY MODELING

A. Overview of The Complete PDE Model

The system dynamics for a Li-ion battery include electrochemical, thermal, electrical, and ageing behaviors across the positive electrode, separator, and negative electrode. A complete battery model that accurately captures spatio-temporal variations of the states and their coupling relationships is schematised in Fig. 1 with comprehensive introduction in [1], [2]. This model is mathematically represented by 17 nonlinear PDEs with the applied current density, $I(t)$, as the system input, and the terminal voltage $V(t)$, SOC, and SOH as the system outputs. Using the definitions in Table I, the system outputs are considered to be:

$$V(t) = \Phi_s^+(L, t) - \Phi_s^-(0, t), \quad (1)$$

$$SOC^\pm(t) = \frac{3}{L^\pm R_p^{3,\pm}} \int_0^{L^\pm} \int_0^{R_p^\pm} \frac{C_s^\pm(x, r, t)}{C_{smax}^\pm} dr dx, \quad (2)$$

$$SOH(t) = 1 - \int_0^{L^-} \frac{Q_{sr}(x, t)}{Q_{max}} dx. \quad (3)$$

It is worth noting that the outputs in (1)-(3) are all finite dimensional whereas the states are infinite dimensional.

B. Stage I: PDE Model Simplification

The system model of Fig. 1 is known to capture battery dynamic characteristics very well [3], [4], [5], but is too complex for most model-based applications including real-time state estimator design. With this in mind, a battery modeling framework is established through a systematic simplification procedure. To deal with the infinite dimensional battery problem, all the PDEs are first reformulated in Hilbert space. Based on the identification of disparate time scales inherent in the battery system, a singular perturbation approach is used to separate the coupled battery states and results in a simplified (reduced) model:

$$\dot{\bar{\mathbf{x}}}_s = \mathcal{F}_s \bar{\mathbf{x}}_s + h_s(\bar{\mathbf{x}}_s, \bar{\mathbf{x}}_f^*, u), \bar{\mathbf{x}}_s(0) = \bar{\mathbf{x}}_{s0}, \quad (4)$$

$$0 = \mathcal{F}_f \bar{\mathbf{x}}_f^* + h_f(\bar{\mathbf{x}}_s, \bar{\mathbf{x}}_f^*, u), \bar{\mathbf{x}}_f(0) = \bar{\mathbf{x}}_{f0}, \quad (5)$$

where $\bar{\mathbf{x}}_f, \bar{\mathbf{x}}_s$ are states in Hilbert space representing the electrical dynamics and the electrochemical, thermal, and ageing phenomena, and $\bar{\mathbf{x}}_f^*$ is the quasi-steady-state of $\bar{\mathbf{x}}_f$. Further details about this PDE model simplification procedure are presented in [2] where the parasitic parameters associated with the electrical states are assumed to be sufficiently small.

By eliminating the fast dynamics with respect to the states $\Phi_s^\pm, \Phi_e^\pm, \Phi_e^{\pm, sep}$, and i_e^\pm , the simplified PDE model has been thus developed with 10 states over x and r spatial dimensions. This model describes the Li-ion concentration requested by SOC calculation in (2) and the capacity fade requested by SOH prediction in (3) will be used for the studies of battery SOC/SOH behavior.

C. Stage II: ODE Model Simplification

An analytical approach has been used in Stage I to separate the multi-time scales within state variables leading to less PDEs in the battery system. For online estimation

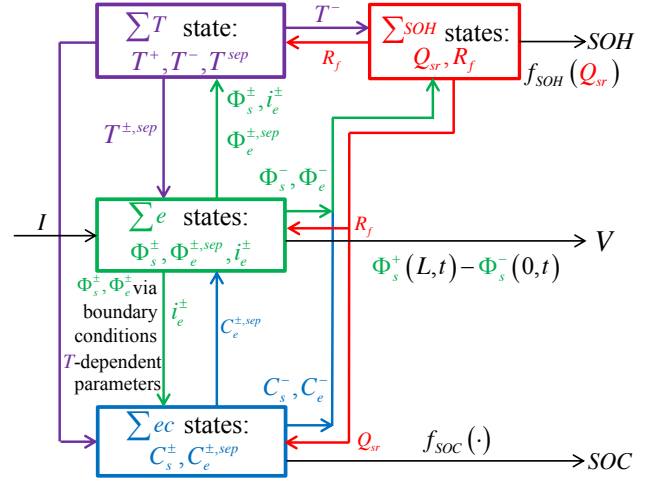


Fig. 1. A complete Li-ion battery model including the system input, outputs, state variables, and coupling relationships among the electrochemical (Σ^{ec}), thermal (Σ^T), electrical (Σ^e), and ageing (Σ^{SOH}) subsystems.

of SOC and SOH, the processors in battery management systems and chargers must be able to compute the internal model accurately and in real-time. However, the infinite dimensional model (4)-(5) is still impractical to implement in such processors. Therefore, further model order reduction with the aid of numerical techniques is explored in this stage.

A straightforward way to reduce this battery model is approximating the PDEs by ordinary differential equations (ODE). This can be realised by finite difference method. The battery states in Euclidian space is $\mathbf{x}(x, r, t)$. Each domain j , *i.e.* the negative electrode, separator, and positive electrode, is discretised into N segments along x -direction with grid resolution obtained as $\Delta x^j = L^j/N$. The discrete state $\mathbf{x}_N^d(i, r, t)$ is assumed to be uniform within the segment i and $i = 1, 2, \dots, N$. The following assumption underlying length scale separation within the battery state variables is introduced:

Assumption 1: Given $\epsilon_1 > 0$, $\exists N^* \in \mathbb{Z}_+$, such that $\forall N \geq N^*$, the states $\mathbf{x}(x, r, t)$ and $\mathbf{x}_N^d(i, r, t)$ satisfy

$$|\mathbf{x}(x, r, t) - \mathbf{x}_N^d(i, r, t)| / |\mathbf{x}(x, r, t)| < \epsilon_1,$$

$$\forall i = 1, \dots, N, \forall t, \text{ and } \forall x \in [(i-1)/L^j, i/L^j].$$

TABLE I
NOMENCLATURE

A, a	cross-sectional area/ specific particle interfacial area
C_s, C_e	Li-ion concentration in solid particles/electrolyte
C_{ss}	Li-ion concentration at the surface of solid particles
D_s, D_e	effective electric/ionic diffusion coefficient
F	Faraday's constant
I, i_e	input current density/local electrolyte current
J	total Li-ion flux
J_I, J_{sr}	Li-ion flux of normal reaction/side reaction
L	total length of the battery cell
M_f	average molecular weight of SEI film
Q_{sr}, Q_{max}	capacity fade/maximum nominal capacity
R, R_f, R_p	universal gas constant/SEI film resistance/radius
Φ_s, Φ_e	electric potential in solid particles/electrolyte
γ	transference number of the anion
μ_e	volume fraction of electrolyte
σ_f, ρ_f	effective conductivity/average density of SEI film
$-, +, sep$	superscript (negative/positive electrode/separator)
x, r	coordinate over thickness/particle radius direction

Remark 1: Assumption 1 is a standard spatial discretisation requirement which implies better approximations of the PDE-system can be obtained with greater numbers of ODEs. As a result, each state in infinite dimension is approximated by N states governed by N ODEs.

Based on Assumption 1, the PDE-based battery model (4)-(5) over the mixed spatial dimensions is approximated by a system of $2N$ PDEs in the domain of (r, t) and $8N$ ODEs only with respect to t . Taking consideration of the computational time costed in the spacial dependency, there is a motivation to further eliminate the r coordinate existed in the states $C_s^+(i, r, t)$ and $C_s^-(i, r, t)$.

The governing equations for the Li-ion concentration diffusion in the negative and positive solid particles are explicitly established as [3]:

$$\frac{\partial C_s^\pm(r, t)}{\partial t} = \frac{D_s^\pm}{r^2} \frac{\partial}{\partial r} \left(r^2 \frac{\partial C_s^\pm(r, t)}{\partial r} \right), \quad (6)$$

subject to boundary conditions

$$\left. \frac{\partial C_s^\pm(r, t)}{\partial r} \right|_{r=0} = 0, \quad (7)$$

$$\left. \frac{\partial C_s^\pm(r, t)}{\partial r} \right|_{r=R_p^\pm} = -\frac{J_I^\pm(t)}{D_s^\pm}, \quad (8)$$

$\forall i \in [1, N]$. For simplification of notation, i has been ignored from (6)-(8) and also in the subsequent analysis.

An analytical solution for (6)-(8) is provided in [16] but involves infinite series such that it is difficult to be directly used for implementation of this battery model. Note that for the derivative of SOC, SOH, and terminal voltage in (1)-(3), only the volume averaged concentration, $C_s(t)$, and surface concentration, $C_{ss}(t)$, in the solid particles are required instead of $C_s(r, t)$ at each position of r . In view of this, the following assumption is employed:

Assumption 2: $\forall \epsilon_2 > 0$ and $\exists n(\epsilon_2, \mathbf{u}) \in \mathbb{Z}_+$ satisfying $\|C_s(r, t) - \hat{C}_s^n(r, t)\|_2 < \epsilon_2$, where $2n$ denotes the order of the polynomial function $\hat{C}_s^n(r, t)$.

Remark 2: A solution for $\hat{C}_s^n(r, t)$ can be obtained by approximating the Li-ion concentration with polynomials in the following form [17]

$$\hat{C}_s^n(r, t) = a_1(t) + a_2(t) \frac{r^2}{R_p^2} + \dots + a_n(t) \frac{r^{2n}}{R_p^{2n}}. \quad (9)$$

By using volume average integration and Assumption 2, the Li-ion diffusion dynamics can be expressed in terms of $C_s(t)$, $C_{ss}(t)$, and volume averaged concentration flux, $q_s(t)$ [17]. Considering the coupling effect between the electrochemical and ageing phenomena, the comprehensive dynamic equations simultaneously describing the solid-phase Li-ion concentration diffusion and consumption for each discrete segment are thus obtained [2], [17]

$$\frac{dC_s^+(t)}{dt} = -\frac{3J_I^+(t)}{R_p^+} \left(1 - \frac{Q_{sr}(t)}{Q_{\max}} \right), \quad (10)$$

$$\frac{dC_s^-(t)}{dt} = -\frac{3J_I^-(t)}{R_p^-}, \quad (11)$$

$$\frac{dq_s^\pm(t)}{dt} = -\frac{30D_s^\pm}{(R_p^\pm)^2} q_s^\pm(t) - \frac{22.5}{(R_p^\pm)^2} J_I^\pm(t), \quad (12)$$

and the surface concentration is a function of the averaged concentration and concentration flux

$$C_{ss}^\pm(t) = C_s^\pm(t) + \frac{8R_p^\pm}{35} q_s^\pm(t) - \frac{R_p^\pm}{35D_s^\pm} J_I^\pm(t). \quad (13)$$

Through (10)-(13), the original PDE battery model is further reduced to an ODE-based model with $12N$ ODEs.

The temperature is a critical factor impacting battery electrochemical and ageing dynamics. However, the interactions within temperature and other battery states render this model as well as model-based estimators computationally expensive to implement. To deal with this issue and also consider practical applications like pure electric vehicles, the following assumptions are applied to the battery system:

Assumption 3: The initial temperature and the end temperature of each cycle satisfy: $T(mt_c) = T((m+1)t_c) = T_0$, $\forall m = 0, 1, \dots, M$, where t_c is the time period for a complete cycle composed of charging, discharging, and relax modes, and M is the cycle number corresponding to a battery's lifetime.

Remark 3: This can be guaranteed when the battery operations start from a constant ambient temperature T_0 , and at the end of each cycle the battery remains relaxed for a sufficiently large time interval such that the battery temperature finally decreases to T_0 .

Assumption 4: In an operating cycle, there exists an $\epsilon_3 > 0$ such that $\forall t \in [mt_c, (m+1)t_c]$,

$$\left| T(t) - \frac{1}{t_c} \int_{mt_c}^{(m+1)t_c} T(t) dt \right| \cdot \frac{1}{T(t)} < \epsilon_3 \ll 1.$$

Remark 4: For a battery with prescribed thermal properties, Assumption 4 can be valid at specified input currents. Inaccuracies caused by approximation of the average temperature can potentially impact temperature-dependent parameters and other states. To check its feasibility, a Taylor series expansion can be used for these nonlinear governing equations. Justification of this assumption will be also shown in forthcoming simulations.

The remaining dynamic equations within this reduced battery model that govern the electrolyte concentration in each electrode, capacity fade, and internal resistance are also explicitly given by:

$$\frac{dC_e^j(i, t)}{dt} = \frac{D_e^j}{\mu_e^j} \frac{C_e^j(i+1, t) - 2C_e^j(i, t) + C_e^j(i-1, t)}{(\Delta x^j)^2} + (\gamma a^j / \mu_e^j) J^j(i, t), \quad (14)$$

$$\frac{dQ_{sr}(i, t)}{dt} = -F a^- A^- L^- J_{sr}(i, t), \quad (15)$$

$$\frac{dR_f(i, t)}{dt} = -\frac{M_f}{\rho_f \sigma_f} J_{sr}(i, t). \quad (16)$$

The total Li-ion flux, $J := J_I + J_{sr}$, can be calculated by the algebraic equations

$$(i_e^\pm(i+1, t) - i_e^\pm(i, t)) / \Delta x^\pm = F a^\pm J^\pm(i, t).$$

Typically the battery ageing has not been modeled during a Li-ion battery's discharging process [5], [18], it is thus known to have $J_{sr} = 0$ in (14)-(16) for discharging periods.

So far, the original PDE-based battery model over two spatial dimensions shown in Fig. 1 has been simplified by using analytical and numerical modeling simplification techniques in succession. As a consequence, an ODE battery model is obtained with $9N$ ODEs representing the system dynamics. And this model with the state vector defined as $\mathbf{x} := [C_s^-, C_s^+, C_e^-, C_e^{sep}, C_e^+, q_s^-, q_s^+, Q_{sr}, R_f]^T$, can also be provided in a compact, generic form

$$\dot{\mathbf{x}} = f(\mathbf{x}, u), \quad (17)$$

$$[\mathbf{y}; \mathbf{z}] = h(\mathbf{x}, u), \quad (18)$$

where the measured output $\mathbf{y} := V$, the unmeasured output $\mathbf{z} := [SOC^-, SOC^+, SOH]^T$, the nonlinear function $f(\cdot)$ can be deduced from (10)-(12), and (14)-(16), and the nonlinear function $h(\cdot)$ is defined by (1), (2), and (3).

To further simplify the course of model-based estimator design, this model (17)-(18) is discretised on temporal domain with Euler method and provided as

$$\mathbf{x}_k = f^d(\mathbf{x}_{k-1}, u_{k-1}), \quad (19)$$

$$[\mathbf{y}_k; \mathbf{z}_k] = h^d(\mathbf{x}_{k-1}, u_{k-1}), \quad (20)$$

where $u(t) = u(k\Delta t) =: u_k, \forall t \in [k\Delta t, (k+1)\Delta t], k \in \mathbb{N}$, and Δt is the sampling period.

D. Model Accuracy

The performance of the developed model (19)-(20) in terms of its modeling accuracy is assessed relative to the initial high-order battery model given in Fig. 1. It is important to note that these open-loop comparisons are not necessarily representative of close-loop estimation capability, but are justifications for the applied modeling reductions and their underlying assumptions.

For validation purposes related to real world vehicle applications, the current data tested from hybrid electric vehicles under the Urban Dynamometer Driving Schedule (UDDS) is used as the system input, as provided in Fig. 2 [7]. To examine the model fidelity at high currents, the original input currents are augmented by a factor of two in the simulations, through which the maximum charging rate has been pushed to 2C-rate. See [1] for the definition of ‘‘C-rate’’ and here 1C corresponds to the input current density of 17.5Ah/m^2 . The value of system input is set up to be negative for charging and positive for discharging. The battery parameters being simulated are adopted from [4], [5] and related to a Li-ion battery with 1.8Ah normal capacity.

To approximately solve the original model of Fig. 1, the numerical methods detailed in our previous work of [19] are employed with the number of discrete segments as 15 for each electrode and separator. Also, in that work, for a given accuracy requirement in capturing battery states, a lookup table ascertaining the relationship between the minimum required spatial grid resolution and operating conditions was provided. Based on the considered system input, here we choose $N=1$ in solving the developed ODE model.

Simulations for two concatenated UDDS driving tests are performed in Modelica with DASSL as the integrator. The

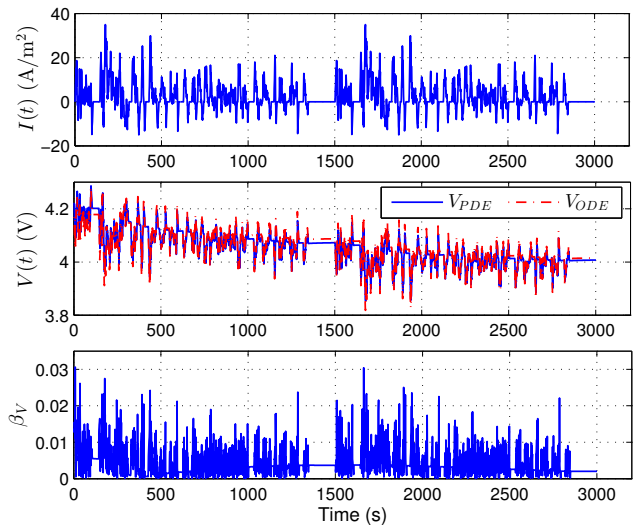


Fig. 2. Comparison of the response of battery terminal voltage between the high-fidelity model and the reduced ODE model under UDDS test with the input $I(t)$.

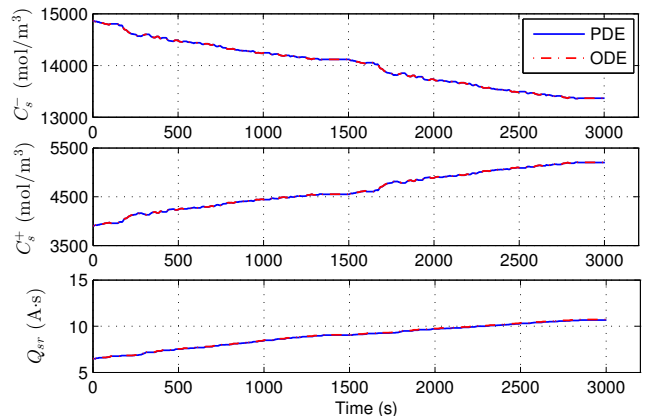


Fig. 3. Comparison of the battery state responses under UDDS test between the high-fidelity model and the developed reduced model.

sampling time is chosen as $\Delta t = 1\text{s}$ which ensures this temporal discretisation error is within 0.01%. The modeling error in terminal voltage is defined as $\beta_V = |V_r - V|/V$, where V_r, V are separately solutions of the reduced model and the high-fidelity model.

Fig. 2 shows the simulation results for terminal voltage under the specified UDDS test. It can be seen that the obtained ODE model closely matches the PDE model in the operating cycle. Specifically, although the error in terminal voltage becomes larger at high charging rates or step input changes, the maximum error of 3% is quite reasonable for most applications. Meanwhile, high fidelity is obtained in predicting battery state dynamics. As given in Fig. 3, the solid-phase Li-ion concentrations, C_s^\pm , and capacity fade, Q_{sr} , that directly relate to SOC and SOH behaviors, are well captured by the developed ODE battery model.

Thus, in the absence of initial error, disturbance, and measurement noise, the proposed reduced model is capable of capturing the key dynamical characteristics for a Li-ion battery. Furthermore, the applied PDE battery model

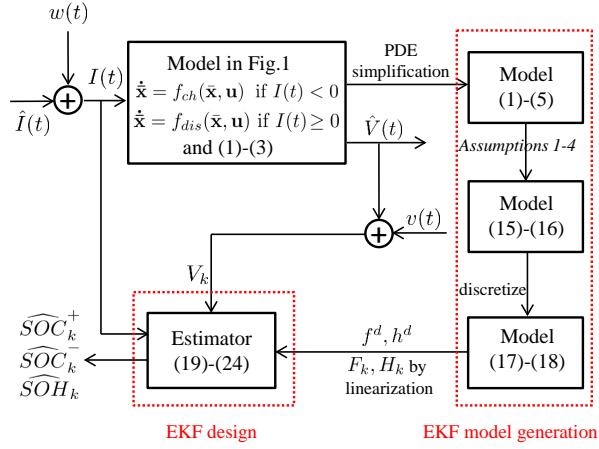


Fig. 4. Schematic of EKF-based SOC and SOH estimation algorithm for a Li-ion battery.

simplification framework and order reduction techniques associated with a set of assumptions are reasonable.

III. SOC & SOH ESTIMATION

In this section, the developed ODE model is used for the estimation of both SOC and SOH for a Li-ion battery.

The complications behind such a problem are mainly attributed to the high nonlinearities involved in both the battery dynamic and output equations and the hybrid model structure for charging and discharging operations given the ageing dynamics have not been considered during discharging stages in the initial battery model. The Kalman filter is an optimal estimator for linear systems with noisy measurements [20]. In order to address these difficulties associated with the battery model, an EKF is designed for online SOC and SOH estimation. In the process, for the calculation of Kalman gain and covariance, the battery model (19)-(20) is successively linearised to a linear time varying (LTV) system. The block diagram provided in Fig. 4 elucidates the comprehensive procedure for EKF model generation and EKF design.

To describe the course of battery SOC and SOH estimator design, $\hat{\mathbf{x}}$ is the estimated state, $\hat{\mathbf{y}}$ and $\hat{\mathbf{z}}$ consist of the estimated outputs, \mathbf{y} is the measured terminal voltage, K is the Kalman gain, P is the estimate covariance, and R, Q are weighting matrices to be tuned for minimising the mean-square state estimate error.

Based on the developed battery model (19)-(20), the following EKF is proposed:

$$\hat{\mathbf{x}}_{k|k} = f^d(\hat{\mathbf{x}}_{k-1|k-1}, u_{k-1}) + K_k(\mathbf{y}_k - \hat{\mathbf{y}}_k), \quad (21)$$

$$[\hat{\mathbf{y}}_k; \hat{\mathbf{z}}_k] = h^d(\hat{\mathbf{x}}_{k|k-1}, u_{k-1}), \quad (22)$$

where, the Kalman gain K_k is calculated from

$$K_k = P_{k|k-1} H_k^T (H_k P_{k|k-1} H_k^T + R)^{-1}, \quad (23)$$

and the estimate covariance P is propagated and updated through (24)-(26) at each time step

$$P_{0|0} = P_0, \quad (24)$$

$$P_{k|k-1} = F_{k-1} P_{k-1|k-1} F_{k-1}^T + Q, \quad (25)$$

$$P_{k|k} = (\mathbf{I} - K_k H_k) P_{k|k-1}. \quad (26)$$

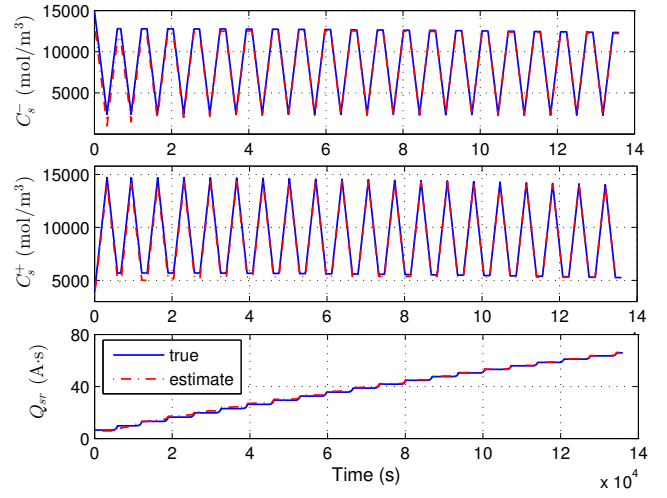


Fig. 5. Evolution of state estimation for the solid-phase Li-concentrations, C_s^- , C_s^+ , and the capacity fade Q_{sr} over 20 cycles.

In (25), F_{k-1} is the Jacobian matrix derived from the nonlinear function f^d based on the previously estimate state $\hat{\mathbf{x}}_{k-1|k-1}$. While, H_k in (26) is the Jacobian matrix derived from the nonlinear function h^d based on the current propagated state $\hat{\mathbf{x}}_{k|k-1}$, and \mathbf{I} is the identity matrix.

This proposed algorithm is then implemented for simultaneous SOC and SOH estimation. By using the input signal u_{k-1} and the previously estimated state $\hat{\mathbf{x}}_{k-1|k-1}$, the state $\hat{\mathbf{x}}_{k|k-1}$ can be predicted based on the nominal battery model. This estimated state is then updated by the voltage measurement \mathbf{y}_k and the calculated Kalman gain K_k . In this simulation investigation, the voltage measurement \mathbf{y}_k is obtained from the “measured” plant, the high-fidelity battery model. Finally, according to (2) and (3), \hat{z}_{SOC-} , \hat{z}_{SOC+} , \hat{z}_{SOH} can be calculated using \hat{x}_1 , \hat{x}_2 , and \hat{x}_8 , respectively.

IV. ESTIMATION RESULTS

Simulations are conducted in this section to examine the designed estimator’s capability for SOC and SOH estimation as compared to the true results derived from the high-fidelity battery model.

The high-fidelity model with noisy input is solved in Modelica associated with Visual C++, providing measured values for the terminal voltage. The numerical methods and parameterization being used are the same as outlined in Section II. While, the EKF based on the derived ODE model is implemented in Matlab.

The battery is charged and discharged at 1C constant current for successive operating cycles. Where the terminal voltage thresholds for charge and discharge operations are set up as 4.15V and 2.9V, respectively. Each cycle is defined for 6800s consisting of charge, discharge, and relax modes to mimic the real world battery utilisation. Zero input current is used during the relax mode. To test the estimator’s capability of capturing the SOH dynamics which have been justified to behave in a slow time scale [2], a long operating time of 20 cycles is chosen. All the states are initialised with 10% relative error, and additional white Gaussian noise with a standard deviation of 80mA/m² is added to the system input.

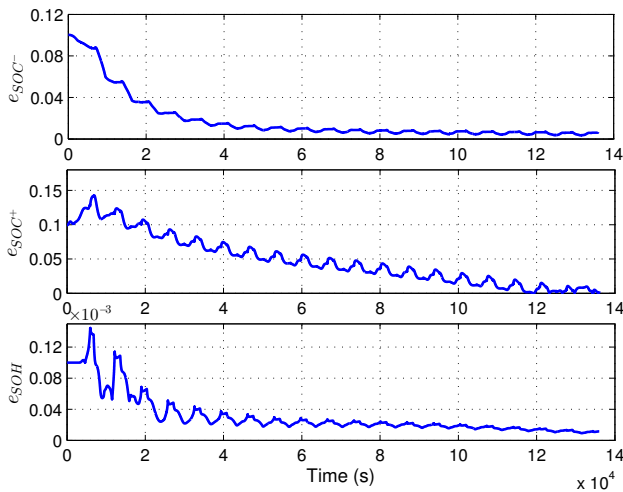


Fig. 6. Estimation results for the negative electrode SOC, positive electrode SOC, and SOH over 20 cycles.

The estimate error for SOC/SOH is defined as $e_z(t) := |z_r(t) - z(t)|/z_0$, where z_r, z are separately the solutions of the ODE model and the PDE model, and the absolute error, $|z_r - z|$, is normalised on its corresponding initial value $z_0 = z(0)$.

The internal states in the battery system are reproduced by the proposed estimator, and estimation results for these critical states, C_s^-, C_s^+ , and Q_{sr} are shown in Fig. 5. It can be seen that the employed EKF is able to quickly compensate the initial deviations added to the states. And all these states closely follow its true value during both the charging and discharging operations.

Fig. 6 depicts the evolution of estimation errors for SOC/SOH. Although large initial errors are assumed to exist in the SOC (10%) and SOH (0.01%) estimation, the state estimator is capable of driving its outputs to converge to the vicinity of the true states. For SOC in the negative and positive electrodes, their steady-state estimation errors are both less than 2%. While, the SOH is also accurately estimated with the steady-state error bounded by 0.001%.

In addition, steady-state errors and periodic error sequences have been observed from Fig. 6. Indeed, exact convergence to the origin for the estimation errors is not possible due to the persistent noise applied to the system input and measurements and model mismatch resulting from model order reductions and successive linearisation. While, the periodic nature of the plant input potentially leads to the periodic variation of error dynamics.

Based on these analysis, the designed estimator for battery SOC/SOH estimation is accurate and robust in dealing with model mismatch, initial errors, and noise.

V. CONCLUSION

In this paper, an EKF-based estimation algorithm synthesised from a physics-based Li-ion battery model is proposed. The employed model was constructively reduced from a high-fidelity PDE battery model by continuously using analytical and numerical reduction techniques. This developed

ODE battery model was shown to efficiently capture the electrochemical and ageing dynamics as compared to the initial high-fidelity model. Through comprehensive simulations, the designed estimator is illustrated to be capable of accurately estimating SOC in both the negative and positive electrodes and SOH using the current and voltage measurements only.

REFERENCES

- [1] C. Zou, C. Manzie, and D. Nešić, "A framework for simplification of PDE-based lithium-ion battery models," *IEEE Trans. Control System Technology*, under review, 2015.
- [2] C. Zou, C. Manzie, and D. Nestic, "PDE battery model simplification for charging strategy evaluation," in *Asian Control Conference*, Kota Kinabalu, Malaysia, 2015, pp. 2355–2360.
- [3] N. A. Chaturvedi, R. Klein, J. Christensen, J. Ahmed, and A. Kojic, "Algorithms for advanced battery-management systems," *IEEE Control System Magazine*, vol. 30, no. 3, pp. 49–68, Jun. 2010.
- [4] W. B. Gu and C. Y. Wang, "Thermal and electrochemical coupled modeling of a lithium-ion cell," *Proc. Electrochemical Society*, vol. 99, pp. 748–762, 2000.
- [5] P. Ramadass, B. Haran, P. M. Gomadam, R. White, and B. N. Popov, "Development of first principles capacity fade model for Li-ion cells," *J. The Electrochemical Society*, vol. 151, no. 2, pp. A196–A203, 2004.
- [6] C. Manzie, C. Zou, and D. Nešić, "Simplification techniques for PDE-based Li-Ion battery models," in *IEEE Conference on Decision and Control*, Osaka, Japan, 2015.
- [7] G. L. Plett, "Extended Kalman filtering for battery management systems of lipb-based hev battery packs: Part 3. state and parameter estimation," *J. Power Sources*, vol. 134, no. 2, pp. 277–292, 2004.
- [8] Y. Zou, X. Hu, H. Ma, and S. E. Li, "Combined state of charge and state of health estimation over lithium-ion battery cell cycle lifespan for electric vehicles," *Journal of Power Sources*, vol. 273, no. 1, pp. 793–803, 2015.
- [9] F. Sun, X. Hu, Y. Zou, and S. Li, "Adaptive unscented Kalman filtering for state of charge estimation of a lithium-ion battery for electric vehicles," *Energy*, vol. 36, no. 5, pp. 3531–3540, 2011.
- [10] B. Saha, K. Goebel, S. Poll, and J. Christophersen, "Prognostics methods for battery health monitoring using a bayesian framework," *IEEE Trans. Instrumentation and Measurement*, vol. 58, no. 2, pp. 291–296, 2009.
- [11] S. Santhanagopalan and R. E. White, "Online estimation of the state of charge of a lithium ion cell," *Journal of Power Sources*, vol. 161, no. 2, pp. 1346–1355, 2006.
- [12] S. Dey and B. Ayalew, "Nonlinear observer designs for state-of-charge estimation of lithium-ion batteries," in *American Control Conference*, 2014, pp. 248–253.
- [13] S. J. Moura, N. A. Chaturvedi, and M. Krstić, "Adaptive partial differential equation observer for battery state-of-charge/state-of-health estimation via an electrochemical model," *Journal of Dynamic Systems, Measurement, and Control*, vol. 136, no. 1, p. 011015, 2014.
- [14] R. Klein, N. A. Chaturvedi, J. Christensen, J. Ahmed, R. Findeisen, and A. Kojic, "Electrochemical model based observer design for a lithium-ion battery," *IEEE Trans. Control System Technology*, vol. 21, pp. 289–302, 2013.
- [15] D. Di Domenico, A. Stefanopoulou, and G. Fiengo, "Lithium-ion battery state of charge and critical surface charge estimation using an electrochemical model-based extended Kalman filter," *Journal of Dynamic Sys., Meas., and Control*, vol. 132, no. 6, p. 061302, 2010.
- [16] H. S. Carslaw and J. C. Jaeger, *Conduction of heat in solids*. Oxford University Press, 1973.
- [17] V. R. Subramanian, V. D. Diwakar, and D. Tapriyal, "Efficient macro-micro scale coupled modeling of batteries," *Journal of The Electrochemical Society*, vol. 152, no. 10, pp. A2002–A2008, 2005.
- [18] G. Ning, R. E. White, and B. N. Popov, "A generalized cycle life model of rechargeable Li-ion batteries," *Electrochimica Acta*, vol. 51, no. 10, pp. 2012–2022, 2006.
- [19] C. Zou, C. Manzie, and S. Anwar, "Control-oriented modeling of a lithium-ion battery for fast charging," in *IFAC World Congress*, Cape Town, South Africa, 2014, pp. 3912–3917.
- [20] R. E. Kalman, "A new approach to linear filtering and prediction problems," *J. Fluids Engineering*, vol. 82, no. 1, pp. 35–45, 1960.